International Scholarly Research Network
ISRN Electronics
Volume 2012, Article ID 359759, 7 pages
doi:10.5402/2012/359759

Research Article

Shaping Resistive Bend Sensors to Enhance Readout Linearity

Giovanni Saggio, Antonino Lagati, and Giancarlo Orengo

Department of Electronics Engineering, Tor Vergata University, Via Politecnico 1, 00139 Rome, Italy

Correspondence should be addressed to Giovanni Saggio, saggio@uniroma2.it

Received 27 September 2012; Accepted 18 October 2012

Academic Editors: J. Abu Qahouq and C. W. Chiou

Resistive bend sensors have been increasingly used in different areas for their interesting property to change their resistance when bent. They can be employed in those systems where a joint rotation has to be measured, in particular biomedical systems, to measure human joint static and dynamic postures. In spite of their interesting properties, such as robustness, low price, and long life, the commercial bend sensors have a response which is not actually linear, as an electronic device to measure bend angles should be, to recover human posture without distortion. In this work, different interfaces for sensor device readout were analyzed and compared from the output response linearity point of view. In order to obtain a sensor characteristic as closer as possible to the ideal linear one, a way to calculate the sensor characteristic with a generalized resistive strip contour, starting from an empiric sheet resistance model, was developed, in order to find what is the more suitable nonuniform geometry.

1. Introduction

In order to measure human body kinematics, it is convenient to adopt sensors, which can measure bending angles with good precision despite a low cost.

Commercial bend sensors are usually made of a few micrometer thick resistive material deposited onto a thicker plastic insulating substrate. The resistive strip is screen printed with a special carbon ink, to be applied on virtually any custom shape and size film [1]. Normally, however, as well as the overall sensor, it has a rectangular geometry. The overall thickness is anyway negligible compared to the total largeness and lengthiness. The ink's resistance value changes with the deflection due to an applied external force. All sensor materials, however, must be able to bend repeatedly without failure for the sensor to work. This type of sensors are available on the market (Images SI Inc. [2], Flexpoint Sensor Systems Inc. [3]). They can be applied to body joint as electronic goniometers, to realize goniometric sock for rotation assessment of body segments in human posture recognition [4–8]. The device sizes can be fitted to each type of joints.

From a characterization point of view, the model which takes into account the mechanical aspect of the sensor predicts a linear behavior of the electric resistive variation with the bending angle [9]. Nevertheless, the sensor resistance has increasing derivatives, especially for small angles, which result in a nonlinear characteristic, as provided by the sensor electrical characterization. However, if the sensor readout is represented by the voltage across an electronic interface rather than its resistance, the sensor resistance characteristic should not be linear in order to achieve a linear response, as it will be demonstrated in the next sections.

In both cases, it could be useful to investigate how to yield the desired sensor characteristic, which allows to obtain an overall linear response. The idea developed in this paper is to change the regular (rectangular) geometry of the resistive strip of the sensor, cutting some part of it, to make the sensor behavior be more linear. This should be possible because the bent section slips with deflection. To this aim, the change of sensor resistance with bending angle was modeled for a generalized resistive strip contour [10].

2. Experimental Apparatus

The apparatus employed for this analysis was designed to emulate, in a controlled environment, the behavior of commercial bend sensors, when applied to body joints, to

Figure 1: Photograph of a 2″ sensor sample in 1 : 1 scale, with a resistive film of $L \times W$ size (Flexpoint Sensor Systems Inc. [3]).

track segment rotations. Figure 1 provides a photo of a sensor strip sample from Flexpoint.

Figure 2 shows a schematic of the experimental set-up. The sensor sample was laid as a cantilever beam on a metal hinge. In order to characterize the sensor behavior with deflection, the sample side connected to the electrodes was locked in a stationary clamp, fixed to a rotating platform operated by a step motor. The other side of the sensor was put in a sliding clamp to avoid the sample stretching. For this type of sensors, the resistive material must be external with respect to the rotation. Bending angle step amplitude was changed reliably with one tenth of degree resolution, from a Labview interface serial connected to a PC. The step motor is a PD-109-57 sample from Trinamic, connected to the PC through a RS-232 cable. The sensor resistance measurement against different bending angles was obtained connecting a digital multimeter to the Labview setup [11].

The characteristics of several commercial bend sensors were measured. In particular, the behavior of three inches long sensors from Flexpoint, when bent on a hinge with a diameter of 8 mm, was investigated. The sensor resistance measurement against deflection angle is plotted in Figure 3(a), as mean and standard deviation results. In Figure 3(b), the normalized mean values are plotted and compared with the ideal linear one, a straight line between 0 and 1.

3. Sensor Readout Interfaces

In this section, the outputs from different sensor readout electronic interfaces are analyzed and compared, especially from the point of view of the degree of linearity in the output voltage response rather than sensor resistance.

For a simple deflection-to-voltage conversion, the bend sensor R_S is tied to a measuring resistor R_M in a voltage divider configuration, as shown in Figure 4. The output of this configuration is described by (1):

$$V_{\text{OUT}} = \frac{V_{\text{REF}}}{1 + R_M/R_S(\phi)}. \tag{1}$$

In the shown configuration, the output voltage increases with increasing deflection. The resistor R_M can be chosen to maximize the desired deflection sensitivity range or the readout linearity. If R_S and R_M are swapped, the output swing decreases with increasing deflection. These two output forms are mirror images about the line $V_{\text{OUT}} = V_{\text{REF}}/2$, therefore this case is not presented here.

A family of V_{OUT} versus deflection curves is shown in Figure 5(a) as it results from (1) for the measured bend sensor device, in a voltage divider configuration, with R_M

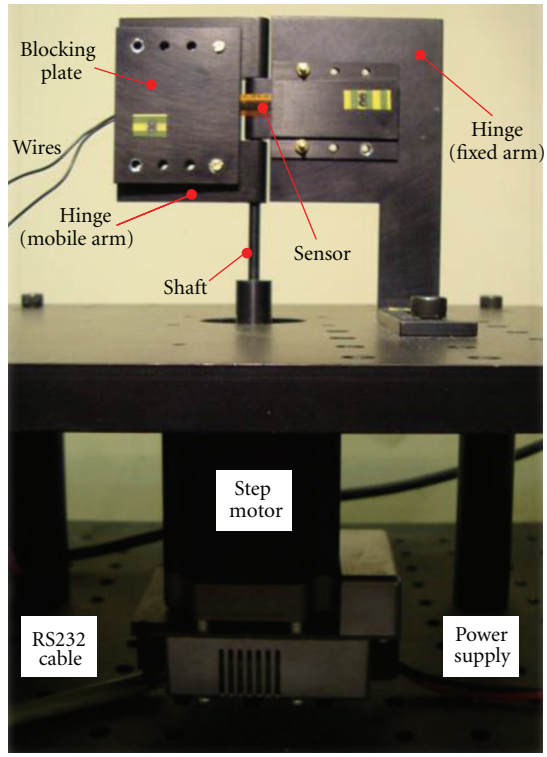

Figure 2: Photograph of the experimental set-up used to characterize the sensor device under test (DUT).

sweeping between the minimum and maximum sensor resistance, for the given deflection range (0 to 120 degrees). A bias voltage V_{REF} of +5 V was used for these examples.

In order to compare the degree of linearity of the output voltage, in Figure 5(b) the normalized curves were plotted, and the distance from the ideal linear one, a straight line between 0 and 1, was calculated as rms error. The result demonstrated that the higher is the R_M resistance, the better is the degree of linearity. In the next section, the chance to decrease the nonlinearity error, shaping the sensor resistive strip, will be investigated.

The same approach was used to analyze the following configurations. In Figure 6, the bend sensor is the input of a resistance-to-voltage converter. A negative reference voltage will yield a positive output swing, from 0 to $+V_{\text{REF}}$, therefore dual sided supplies are necessary. The output of this amplifier is described by

$$V_{\text{OUT}} = -V_{\text{REF}} \frac{R_M}{R_S(\phi)}, \tag{2}$$

where the output is inversely proportional to the bend sensor resistance. Changing R_M and/or V_{REF} changes the response slope, as it can be seen in Figure 7(a). However R_M should be chosen to obtain a full swing, from 0 to $+V_{\text{REF}}$, given the maximum deflection to measure for each particular bend sensor application.

The drawback of this configuration is that, sweeping the resistance R_M, all the output voltages characteristics

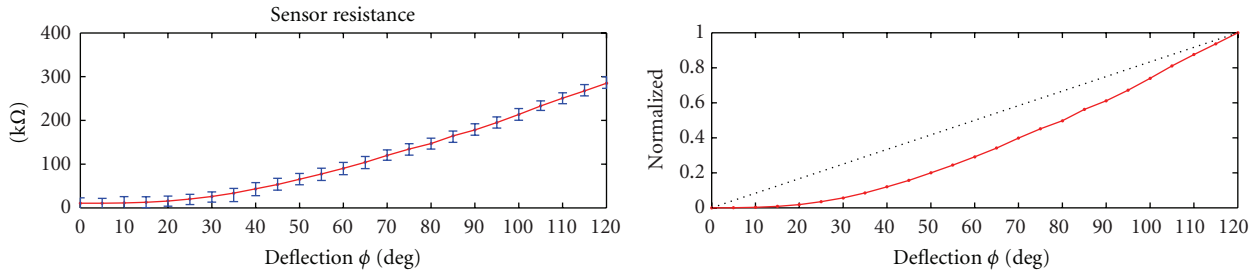

(a) (b)

Figure 3: Sensor resistance static characterization (a) as mean and standard deviation, and the normalized mean (b) compared with the ideal linear one (dotted).

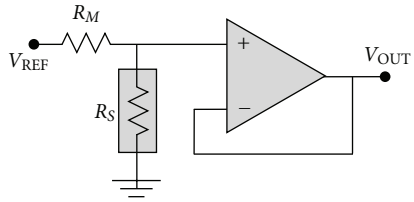

Figure 4: Sensor readout with a voltage divider.

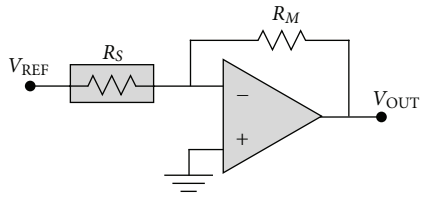

Figure 6: Resistance-to-voltage converter.

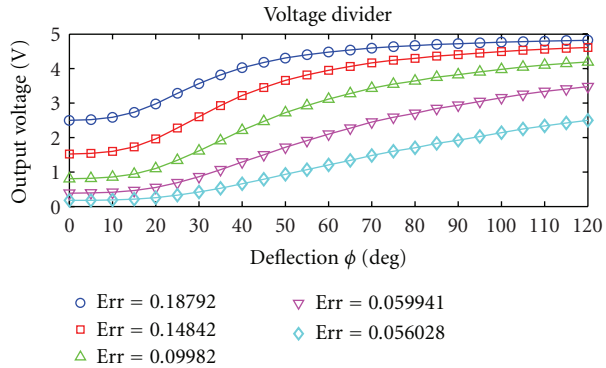

(a)

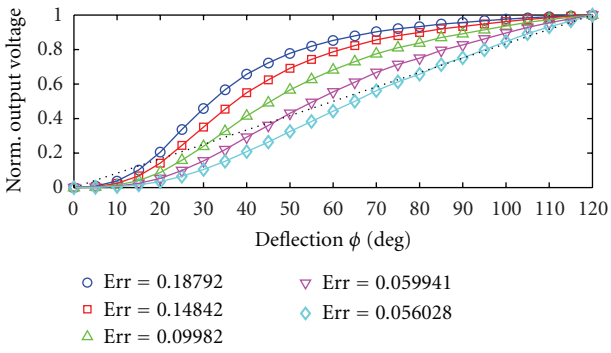

(b)

Figure 5: Measured output voltage sweeping R_M (a) and the corresponding normalized ones (b), compared with an ideal linear characteristic (dotted), for a simple voltage divider. The most linear one corresponds to the bold markers. The total nonlinearity error is also reported for each normalized trace.

correspond to the same normalized one, in addition very far from the ideally linear one, as it can be seen in Figure 7(b).

Unfortunately, the same conclusions can be also drawn for the following readout interface, depicted in Figure 8, which are slightly modified versions of the resistance-to-voltage converter detailed in Figure 6, described by (3) and (4), respectively:

$$V_{OUT} = \frac{V_{REF}}{2}\left[1 - \frac{R_M}{R_S(\phi)}\right], \tag{3}$$

$$V_{OUT} = \frac{V_{REF}}{2}\left[1 + \frac{R_M}{R_S(\phi)}\right]. \tag{4}$$

In the circuit (a), the output swing is from $V_{REF}/2$ to 0 V. In the case where R_M is greater than R_S, the output will go into negative saturation. In the circuit (b), the output swing is from $V_{REF}/2$ to V_{REF}. In the case where R_M is greater than R_S, the output will go into positive saturation. Both designs yield one-half the output swing of the previous circuit, but only require single-sided supplies and positive reference voltages. However, the same result of the previous case, in terms of linearization, was obtained.

In summary, only the first configuration, shown in Figure 4, allows a suitable choice of the measurement resistance R_M, to obtain the most linear output voltage characteristic.

In the rest of this paper, the possibility to modify the sensor characteristic, to obtain a more linear behavior for the resistance or the output voltage, will be investigated, because the accuracy of output measurements, both in terms of resistance or voltage, can be affected by the output nonlinearity. When bend sensor are applied, in fact,

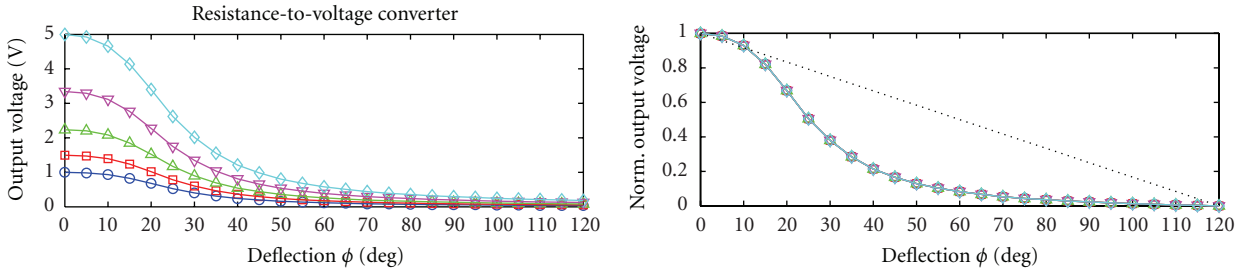

(a) (b)

Figure 7: Measured output voltage sweeping R_M (a) and the superposition of the normalized ones (b), compared with an ideal linear characteristic (dotted), for a resistance-to-voltage converter.

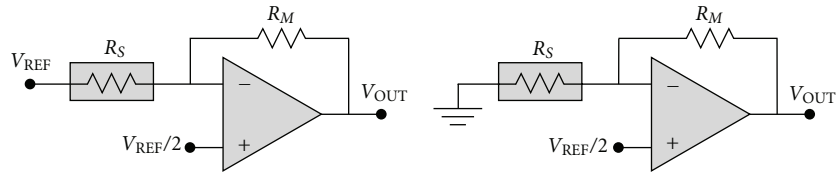

(a) (b)

Figure 8: Additional resistance-to-voltage converters.

the measurement device needs to be calibrated each time. If the sensor would perform a linear response, the calibration procedure can be limited to measure the extreme points on the measurement interval, then interpolating them along a straight line. When a nonlinear response occurs, indeed, the calibration procedure is more complex.

For the easiness of realization, to attempt a linearity enhancement, shaping the geometry of sensor resistive strip, it represents an interesting challenge.

4. Sensor Resistance Modeling

As a preliminary step of the sensor geometry analysis, a reliable model for its sheet resistance or resistance per square, against both deflection and variation of the resistive strip geometry, must be defined.

For a flat rectangular sensor of size $L \times W$, where L is the length and W the width of the resistive strip, its constant sheet resistance $R^{0^\circ}_{\text{sheet}}$ and its total resistance $R^{0^\circ}_S$ are linked by

$$R^{0^\circ}_s = R^{0^\circ}_{\text{sheet}} \frac{L}{W}. \tag{5}$$

If the resistive strip does not have a rectangular contour, say not a constant width, given by the function $w(x)$, the total resistance can be numerically calculated from the equation

$$R^{0^\circ}_s = R^{0^\circ}_{\text{sheet}} \sum_{i=1}^{N} \frac{\Delta x_i}{w(x_i)}, \tag{6}$$

where the strip length was divided into N uniform or non-uniform segments of length Δx_i for numerical integration.

As previously affirmed, when the substrate is bent, the material of its resistive strip is stretched, and the sheet resistance increases around the bending axis. Although it is rather difficult to physically model this phenomenon, an empirical model can be still attempted with a general Gaussian function, symmetrical with respect to the rotation axis, supposed at a known distance L_R from the strip longitudinal edge at $x = 0$. The Gaussian function,

$$G(x) = \frac{1}{\sqrt{2\pi\sigma^2}} e^{-(x)^2/(2\sigma^2)}, \tag{7}$$

was chosen for its useful property according to

$$\int_{-\infty}^{+\infty} G(x)dx = 1. \tag{8}$$

The global sheet resistance then results from

$$R_{\text{sheet}}(x, \phi) = R^{0^\circ}_{\text{sheet}} + K(\phi) G(x - L_R), \tag{9}$$

where the unknown parameters are the calibration factor $K(\phi)$, scaling the sheet resistance with the bending angle ϕ, and the variance σ, which determines the longitudinal extension of the region around the bending axis, where the resistivity increases. By comparison of the model simulation and experimental results, to this parameter it was assigned a constant value $\sigma = d/2$, where d is the hinge diameter. Then, the resistance variation of a rectangular sensor with the bending angle can be calculated as

$$\begin{aligned} R_S(\phi) &= \frac{1}{W} \sum_{i=1}^{N} R_{\text{sheet}}(x_i, \phi) \Delta x_i \\ &= R^{0^\circ}_S + \frac{K(\phi)}{W} \sum_{i=1}^{N} G(x_i - L_R) \Delta x_i, \end{aligned} \tag{10}$$

from which results

$$R_S(\phi) = R_S^{0^\circ} + \frac{K(\phi)}{W}, \tag{11}$$

standing that, if the most of the Gaussian function is inside the strip length, results from (8)

$$\sum_{i=1}^{N} G(x_i - L_R)\Delta x_i \simeq 1. \tag{12}$$

Equation (11) allows to determine the calibration factor $K(\phi)$, from measurements of the sensor resistance against deflection, for a rectangular sensor, as

$$K(\phi) = W\left[R_{S\_\text{rect}}(\phi) - R_S^{0^\circ}\right]. \tag{13}$$

It is worth to note that the calibration factor, even if calculated for a rectangular strip, is independent from the strip geometry. Then, the response of a nonuniform geometry can be calculated from

$$R_S(\phi) = \sum_{i=1}^{N} \frac{R_{\text{sheet}}(x_i, \phi)}{w(x_i)}\Delta x_i, \tag{14}$$

$$\begin{aligned} R_S(\phi) &= R_{\text{sheet}}^{0^\circ} + K(\phi)\sum_{i=1}^{N} G(x_i - L_R)\frac{\Delta x_i}{w(x_i)} \\ &= R_S^{0^\circ} + K(\phi)\cdot H_{\text{geom}}, \end{aligned} \tag{15}$$

where H_{geom} is a constant factor dependent on sensor geometry, but independent from the bending angle. As a consequence, since $K(\phi)$ is linearly dependent from the characteristic of a rectangular sensor strip $R_{S\_\text{rect}}(\phi)$, as it results from (13), then the normalized sensor resistance, with nonuniform geometry, is the same of that derived from the characteristic of a rectangular one, given by (10). In other words, no linearity enhancement can be yield from nonuniform geometry in this case.

So far, however, it has not been taken into account that, when the sensor is bent, the sample side not connected to the electrodes slides in a clamp of an amount equals to the arc of the hinge (diameter d) corresponding to the rotation angle, and the position of the symmetry axis for the Gaussian model moves away from the locked edge ($x = 0$) of half this quantity, namely,

$$s(\phi) = \frac{1}{2}\frac{\phi}{180^\circ}\frac{\pi d}{2}, \tag{16}$$

from which the sheet resistance results

$$R_{\text{sheet}}(x, \phi) = R_{\text{sheet}}^{0^\circ} + K(\phi)\cdot G[x - L_R - s(\phi)]. \tag{17}$$

To keep the rotation axis in the central region of the strip, a good practice would be to set

$$L_R = 0.5(L - s_{\max}). \tag{18}$$

Calculating the total sensor resistance

$$R_S(\phi) = R_S^{0^\circ} + K(\phi)\sum_{i=1}^{N} G[x_i - L_R - s(\phi)]\frac{\Delta x_i}{w(x_i)}, \tag{19}$$

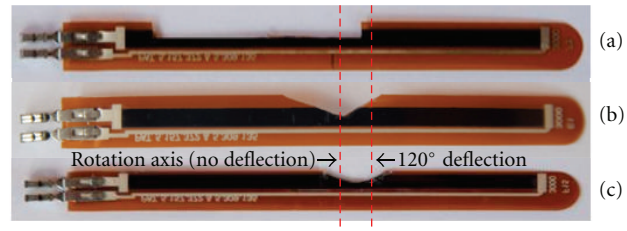

Figure 9: Three inch Flexpoint sensor samples, with cuttings of rectangular (a), triangular (b), and circular (c) shape, randomly optimized for the most linear voltage, in the voltage divider readout interface of Figure 4.

it can be also expressed as

$$R_S(\phi) = R_S^{0^\circ} + K(\phi)\cdot H_{\text{geom}}(\phi), \tag{20}$$

where, this time, the geometric factor $H_{\text{geom}}(\phi)$ is dependent on the bending angle. Finally, in this case, the normalized sensor resistance has a different behavior between uniform and nonuniform geometry. This fact will be exploited in the next section to investigate if particular geometries can lead to a linearization of the sensor intrinsic nonlinear behavior.

5. Sensor Linearity Enhancement

In this section, the optimization of the resistive strip geometry, to yield a more linear behavior with deflection, is investigated from two points of view, that is, a more linear sensor resistance, in one case, and a more linear readout, as output of the voltage divider of Figure 4, in the other case.

However, it is to note that the highest nonlinearity is observed for small angles, where the sheet resistance has a little increase. As a consequence, the modulation of the sensor width has a little influence on its performance for small deflections. Nevertheless, a geometry optimization was attempted, investigating different simple cuttings of the original sensor strip, in particular of rectangular, triangular, and circular shape, where dimensions were randomly optimized, on the basis of the rms error (nonlinearity error) between the normalized sensor performance and an ideal linear one. This approach was attempted on the three inch sensors from Flexpoint, where the original rectangular strip size was 61 × 2.8 mm.

Using the sheet resistance model defined in the previous section, two separate random optimizations were performed, sweeping geometry parameters, to optimize the linearity of the normalized resistance, from one hand, and the linearity of the readout voltage from the voltage divider of Figure 4, from the other hand. In the last case, moreover, the measurement resistance R_M was swept, at each iteration, inside the sensor resistance dynamic, to yield the most linear behavior, in terms of readout voltage, as already done in Figure 5.

Figure 9 shows the photograph of the sensor strip cuttings, as a result of geometry random optimization, attempted

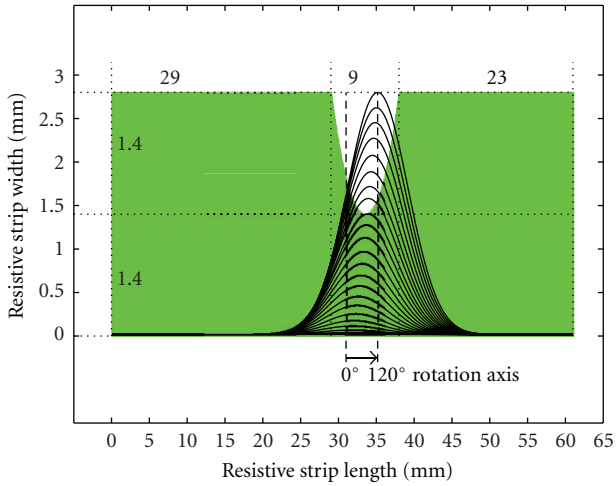

Figure 10: Randomly optimized resistive strip circular contour for the most linear readout voltage. The sheet resistance Gaussian model is also plotted, with the slide of the rotation axis under deflection.

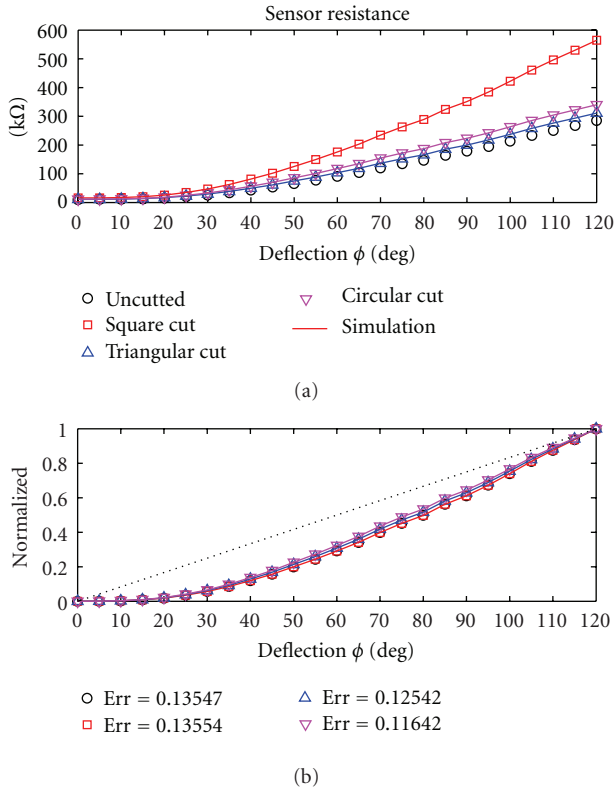

Figure 11: Comparison between sensor resistance (a) and its normalized value (b) against deflection, for rectangular, triangular, and circular contour shape, randomly optimized for the most linear sensor resistance.

for rectangular, triangular, and circular shapes, with the target to yield the most linear sensor voltage in the voltage divider readout interface.

The result of random optimization of the strip contour, with a circular shape, is reported in Figure 10, where the

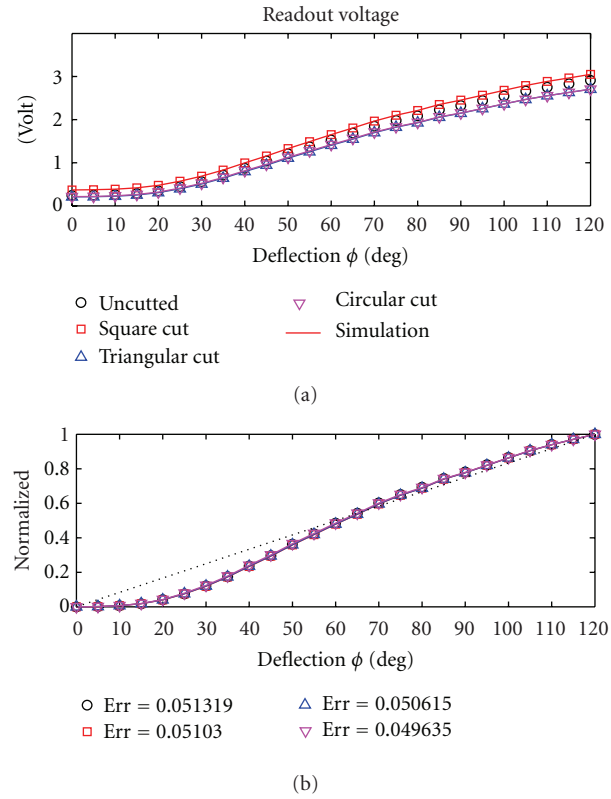

Figure 12: Comparison between sensor voltage from a voltage divider readout interface (a) and its normalized value (b) against deflection, for rectangular, triangular, and circular contour shape, randomly optimized for the most linear readout voltage.

calibrated sheet resistance Gaussian models, and their shift with deflection, were superimposed.

Results for each cutting shape are reported in Figures 11 and 12, respectively, for the target of sensor resistance and readout voltage linearity enhancement. From comparison of the rms nonlinearity error, the cut of circular shape reached the best performance in both cases. This demonstrated that some linearity improvement can be obtained, except for small deflection angles.

This results can be furtherly improved if geometry optimization will be attempted without layout constraints, that is, allowing a larger resistive film. However, standing that the film resistivity changes slightly for small deflection angles, it will be hard to enhance sensor sensitivity in this case.

6. Conclusions

The linearization of the bend sensor's characteristic leads to undeniable advantages in joint rotation assessment. In this work, an empiric model for the sensor sheet resistance variation with deflection is proposed, and a method to calculate the total sensor resistance for any resistive strip geometry is described. This approach was applied to compare some resistive strip cuttings of different shapes and sizes, in order to enhance the sensor response linearity, as

resistance or output voltage in the chosen readout circuit. Results demonstrated that some linearity improvement can be obtained, except for small deflection angles.

References

[1] G. Latessa, F. Brunetti, A. Reale, G. Saggio, and A. Di Carlo, "Piezoresistive behaviour of flexible PEDOT:PSS based sensors," *Sensors and Actuators B*, vol. 139, no. 2, pp. 304–309, 2009.

[2] Images SI Inc., Staten Island NY, USA.

[3] "Flexpoint Sensor Systems Inc.," South Draper UT, USA.

[4] R. Gentner and J. Classen, "Development and evaluation of a low-cost sensor glove for assessment of human finger movements in neurophysiological settings," *Journal of Neuroscience Methods*, vol. 178, no. 1, pp. 138–147, 2009.

[5] L. Dipietro, A. M. Sabatini, and P. Dario, "A survey of glove-based systems and their applications," *IEEE Transactions on Systems, Man and Cybernetics C*, vol. 38, no. 4, pp. 461–482, 2008.

[6] L. K. Simone, N. Sundarrajan, X. Luo, Y. Jia, and D. G. Kamper, "A low cost instrumented glove for extended monitoring and functional hand assessment," *Journal of Neuroscience Methods*, vol. 160, no. 2, pp. 335–348, 2007.

[7] N. W. Williams, J. M. T. Penrose, C. M. Caddy, E. Barnes, D. R. Hose, and P. Harley, "A goniometric glove for clinical hand assessment. Construction, calibration and validation," *Journal of Hand Surgery*, vol. 25, no. 2, pp. 200–207, 2000.

[8] N. M. Noaman, A. R. Ajel, and A. A. Issa, "Design and implementation of DHM glove using variable resistors sensors," *Journal of Artificial Intelligence*, vol. 1, no. 1, pp. 44–52, 2008.

[9] G. Saggio, "Mechanical model of flex sensors used to sense finger movements," *Sensors and Actuators A*, vol. 185, pp. 53–58, 2012.

[10] G. Saggio, S. Bocchetti, C. A. Pinto, G. Latessa, and G. Orengo, "Non uniform geometry bend sensors exploited for biomedical systems," in *Proceedings of the International Conference on Bio-Inspired Systems and Signal Processing (BIOSIGNALS '11)*, pp. 389–392, Rome, Italy, January 2011.

[11] G. Saggio, M. De Sanctis, E. Cianca, G. Latessa, F. De Santis, and F. Giannini, "Long term measurement of human joint movements for health care and rehabilitation purposes," in *Proceedings of the 1st International Conference on Wireless Communication, Vehicular Technology, Information Theory and Aerospace and Electronic Systems Technology (Wireless VITAE '09)*, pp. 674–678, Aalborg, Denmark, May 2009.